

# An innate twist between Crick's wobble and Watson-Crick base pairs

PRAKASH ANANTH, GUNASEELAN GOLDSMITH, and NARAYANARAO YATHINDRA<sup>1</sup>

Institute of Bioinformatics and Applied Biotechnology, Bangalore 560100, Karnataka, India

## ABSTRACT

Non-Watson-Crick pairs like the G·U wobble are frequent in RNA duplexes. Their geometric dissimilarity (nonisostericity) with the Watson-Crick base pairs and among themselves imparts structural variations decisive for biological functions. Through a novel circular representation of base pairs, a simple and general metric scheme for quantification of base-pair nonisostericity, in terms of residual twist and radial difference that can also envisage its mechanistic effect, is proposed. The scheme is exemplified by G·U and U·G wobble pairs, and their predictable local effects on helical twist angle are validated by MD simulations. New insights into a possible rationale for contextual occurrence of G·U and other non-WC pairs, as well as the influence of a G·U pair on other non-Watson-Crick pair neighborhood and RNA-protein interactions are obtained from analysis of crystal structure data. A few instances of RNA-protein interactions along the major groove are documented in addition to the well-recognized interaction of the G·U pair along the minor groove. The nonisostericity-mediated influence of wobble pairs for facilitating helical packing through long-range interactions in ribosomal RNAs is also reviewed.

**Keywords:** non-Watson-Crick pairs; wobble pairs; nonisosteric base pairs; self-isosteric base pairs; residual twist; radial difference

## INTRODUCTION

Watson-Crick (WC) base pairs have dominated the double helical landscape ever since the elucidation of the structure of DNA. Although the four bases with their characteristic distribution of hydrogen bond donors and acceptors offer a variety of base-pairing interactions, WC pairs are singularly inimitable, due to their implicit geometrical equivalence and self-isostericity, conferring a unique and distinct ability of interchangeability of paired bases quintessential for uniform duplex. Unlike DNA, RNA duplexes are not composed entirely of WC base pairs. Base pairs other than the WC prevail in the RNA world.

Among the many non-WC (nWC) pairs that occur in RNA, the G·U wobbles have attracted greater attention because of their abundance, next only to WC pairs, and due to their biological implications (Strobel and Cech 1995; Hermann and Westhof 1999; Masquida and Westhof 2000; Varani and McClain 2000). The G·U pair was one of the first nWC pairs proposed by Crick to account for the degeneracy of the genetic code (Crick 1966). Structural investigations of yeast tRNA<sup>Phe</sup> (Ladner et al. 1975; Quigley et al. 1975; Stout et al. 1976) revealed a G·U wobble pair held together by two hydrogen bonds. The characteristic hydrogen

bonding pattern renders the glycosidic bond angles at G ( $\lambda_G = 40^\circ$ ) and at U ( $\lambda_U = 65^\circ$ ) to be unequal, making  $\lambda$  distinctive from those seen for WC base pairs. This forms the origin of its nonisostericity with WC pairs and non-self-isostericity within the G·U pair. Such and other types of subtle but distinguishing geometric variations among nWC pairs contribute to their nonisostericity and limit their replacement, either with WC pairs or with other nWC pairs, especially in a WC pair-dominated duplex, without entailing deformations of RNA duplex. Presence of such nonisosteric base interruptions in a WC duplex may also result in unique structural traits for nWC pairs to serve as recognition elements.

Diversity of nWC base pairs and their significance began to emerge with the elucidation of structures of RNA systems. Every new RNA structure offered insights into the effects of nWC pairs on structural, functional, and thermodynamic stability of the WC pair dominant duplex. Efforts to systematically characterize different nWC base pairs have resulted in various classification and nomenclature schemes (Saenger 1984; Leontis and Westhof 2001; Nagaswamy et al. 2002; Lee and Gutell 2004). However, precise understanding of their possible mechanistic influence warrants quantification of their unique geometric properties particularly in comparison with WC pairs. We propose here a simple metric scheme to characterize nonisostericity between any two base pairs in general. It has the intrinsic merit to anticipate the effects of base-pair nonisostericity. We demonstrate this by identifying an

<sup>1</sup>Corresponding author  
E-mail [yathindra@ibab.ac.in](mailto:yathindra@ibab.ac.in)

Article is online at <http://www.rnajournal.org/cgi/doi/10.1261/rna.036905.112>.

innate residual twist as the critical geometrical feature that renders G·U and U·G pairs to be nonisosteric with WC pairs and further predict its influence in terms of local under- or overwinding in a RNA duplex, in striking accord with experimental observations.

### CIRCULAR REPRESENTATION TO CHARACTERIZE ISOSTERICITY AND NONISOSTERICITY OF BASE PAIRS

The isosteric or nonisosteric nature between any two base pairs can be described by overlaying base pairs encompassed by circles formed with C1' ... C1' atoms as the diameter, since physical context of isostericity/nonisostericity becomes readily apparent through such circular representations. Superposition of A·U, U·A, G·C, and C·G WC pair circles (Fig. 1A) results in a near-perfect alignment, especially the line joining their C1' ... C1' atoms. Interchange of U and A within A·U and G and C within a G·C pair retains isosteric features, rendering them to be also self-isosteric. In sharp contrast, overlaying a G·U pair on a G·C base pair (a representative of a WC pair) reveals that the line joining the C1' ... C1' atoms of the G·U pair does not align with the line joining the C1' ... C1' atoms of the G·C pair but subtends a counter-clockwise twist of +14° (Fig. 1B). We define this innate twist as the residual twist ( $\Delta t^\circ$ ) since it appears even prior to effecting the prescribed twist ( $t = 33^\circ$  for an ideal ARNA) required to generate a helical structure. Thus, the G·U pair is

nonisosteric with the WC pair, and the degree of nonisostericity is equivalent to  $\Delta t$ . On the contrary, when a U·G base pair follows a WC pair, it subtends a clockwise twist, defining a negative residual twist of  $\Delta t \approx -11^\circ$  (Fig. 1C). This difference in the magnitude as well as direction of  $\Delta t$  compared to the G·U pair (Fig. 1B) is because of the fact that G·U and U·G base pairs are not interchangeable ( $G \cdot U \neq U \cdot G$ ), an attribute arising out of the nonequivalent glycosidic bond angles ( $\lambda_G \neq \lambda_U$ ). This lack of self-isostericity in the G·U and U·G wobble pair differentiates them from each other as well as from self-isosteric WC pairs. By the same arguments, superpositions of U·G and G·U pairs (5' U·G/G·U 3') and G·U and U·G pairs (5' G·U/U·G 3') display strikingly large nonisostericity characterized by  $\Delta t \approx +24.9^\circ$  and  $\Delta t \approx -24.9^\circ$ , respectively (Fig. 1D,E).

Further, the C1' ... C1' separations (diameters of the encompassing circles) of G·U and WC pairs are not precisely identical but exhibit very small differences (Fig. 1B). This is expressed through the radial difference ( $\Delta r$  Å). A radius higher than the preceding reference pair (G·C, in this case) is defined as positive ( $+\Delta r$ ), and lower, as negative ( $-\Delta r$ ). It may be readily surmised that positive and negative  $\Delta r$  might cause bulges or constrictions, respectively, in a duplex. Incidentally, the radial difference between G·U (U·G) and WC pairs is negligibly small (0.05 Å) and is, therefore, expected to exert little influence. Seemingly then, the magnitude and the sign of  $\Delta t$  are adequate to describe nonisostericity between Crick's wobble and WC pairs.

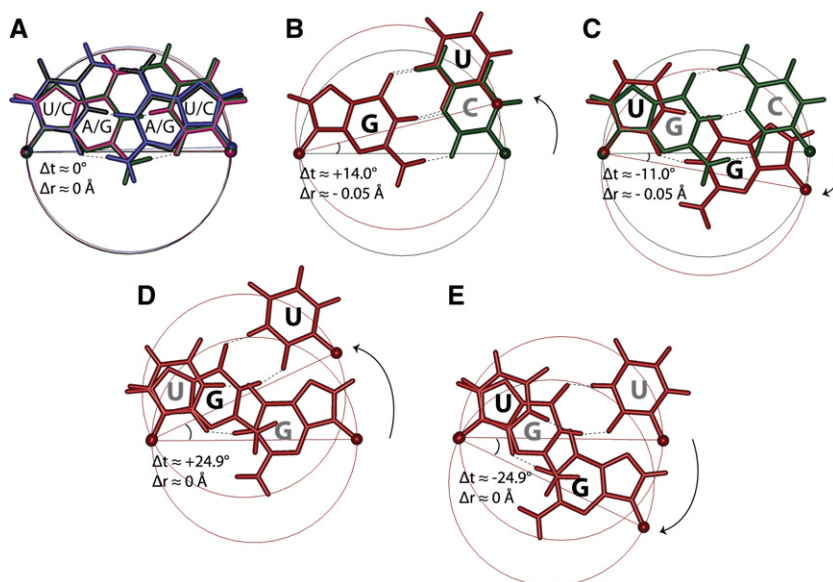


**FIGURE 1.** Superposition of base pairs in their circular representations. (A) Self-isosteric WC pairs (G·C, C·G, A·U, U·A), (B) G·U pair on the 3' side of a G·C pair (a representative of a WC pair), (C) U·G pair on the 3' side of a G·C pair, (D) G·U pair on the 3' side of a U·G pair, and (E) U·G pair on the 3' side of a G·U pair. Each WC and nWC base pair is encompassed by a circle with the respective C1' ... C1' separation as the diameter. C1' atoms are shown by filled circles and hydrogen bonds by dotted lines. A representative WC pair (G·C) is colored green, while G·U and U·G are colored brown. Note the overwinding and underwinding effect that can be readily inferred by the counter-clockwise and clockwise movement of the red circles indicated by arrows.

### MECHANISTIC INFLUENCE OF NONISOSTERICITY ( $\Delta t$ )

It does not entail much reason to foretell from above that one of the mechanistic effects of residual twist between G·U and WC pairs would be in the form of influencing the local helical twists (Fig. 2). Accordingly, a G·U wobble pair succeeding a WC pair in a RNA duplex is expected to experience an effective helical twist of  $t + \Delta t$  ( $33^\circ + 14.0^\circ \approx 47.0^\circ$ ), while that preceding a WC pair experiences a helical twist of  $t - \Delta t$  ( $33^\circ - 14^\circ \approx 19^\circ$ ) (Table 1).

On the other hand, the influence of a U·G pair would be opposite to that of a G·U pair (Table 1; Fig. 1C) in view of the non-self-isosteric nature of G·U and U·G pairs resulting in their opposite effect on the direction of  $\Delta t$ . Thus, a U·G pair succeeding a WC pair would experience an effective helical twist of  $t - \Delta t$  ( $33^\circ - 11^\circ \approx 22^\circ$ ), while the same preceding a WC pair would experience an effective twist of  $t + \Delta t$  ( $33^\circ + 11^\circ \approx 44^\circ$ ) in a RNA duplex. Therefore, a U·G or G·U

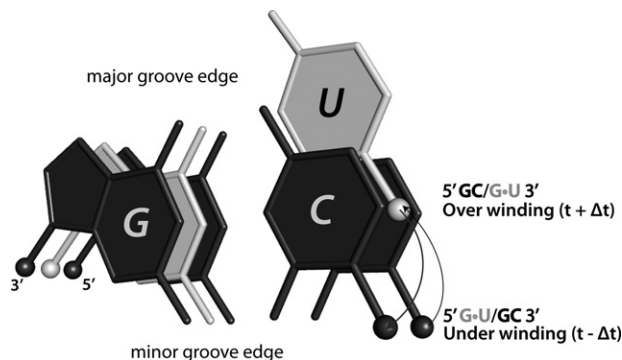


**FIGURE 2.** Illustration of the mechanistic effects of base-pair nonisostericity (residual twist) between WC and Crick's wobble base pairs. A G·U wobble pair (gray) flanked on either side by G·C base pairs (black) when the helical twist  $t = 0^\circ$ . Note the complete overlap of guanines and protrusion of uracil of the intervening G·U pair toward the major groove edge. The central G·U wobble subtends a counter-clockwise and clockwise twist with respect to the preceding and succeeding cytosine (along the direction of helical propagation), depicted by arrows. This results in a positive ( $\Delta t = +14^\circ$ ) and negative ( $\Delta t = -14^\circ$ ) residual twist manifesting as a local helical overwinding ( $33^\circ + 14^\circ = 47^\circ$ ) and local helical underwinding ( $33^\circ - 14^\circ = 19^\circ$ ) at the 5' G·C/G·U 3' and 5' G·U/G·C 3' steps, respectively, in the presence of a helical twist angle of  $33^\circ$ .

wobble pair would induce a mechanistic influence in the form of local underwinding or overwinding. Most significantly, the negative and positive values of  $\Delta t$  directly correlate with underwinding and overwinding of the helical twist, respectively, enabling a straightforward understanding of the effect of base-pair nonisostericity.

### VALIDATION OF PREDICTED MECHANISTIC EFFECTS OF $\Delta t$

In order to verify the predicted mechanistic effects of  $\Delta t$ , molecular dynamics (MD) simulations (20 nsec using AMBER 11.0) (Case et al. 2010) of RNA duplexes comprising G·U and U·G wobble pairs under different sequence contexts (Scheme A) have been performed. Excellent agreement (Fig. 3) between the predicted helical twist angles based on the concept of residual twist, MD simulations, and crystal structure data supports the usefulness of the present scheme of defining nonisostericity between base pairs.

MD simulation and X-ray crystal structure data suggest an average helical twist angle of  $39.4^\circ$  and  $36.2^\circ$  (overwinding), respectively, at the WC/G·U base step, and  $24^\circ$  and  $28.2^\circ$  (underwinding), respectively, at the G·U/WC base step (Scheme A1; Fig. 3A). This trend nearly reverses with the average twist angles of  $26.4^\circ$  and  $28.7^\circ$  (underwinding) at the WC/U·G base step, and  $39.6^\circ$  and  $37.4^\circ$  (overwinding) at the U·G/WC base step (Scheme A2; Fig. 3B). In conformity with the above, a trend of underwinding (MD =  $25.8^\circ$ , X-ray =  $27.9^\circ$ ), overwinding (MD =  $39.8^\circ$ , X-ray =  $37.1^\circ$ ), and underwinding (MD =  $25.6^\circ$ , X-ray =  $28.2^\circ$ ) is observed (Fig. 3C) at the GU, UG, and GC steps, respectively, when a UG dinucleo-

tide intervenes in a WC paired duplex (Scheme A3). Exactly the reverse pattern occurs at the GG, GU, and UC base steps (Fig. 3D), exhibiting overwinding (MD =  $39.3^\circ$ , X-ray =  $36.4^\circ$ ), underwinding (MD =  $25.4^\circ$ , X-ray =  $27.8^\circ$ ), and overwinding (MD =  $38.8^\circ$ , X-ray =  $36.9^\circ$ ), respectively, in a GU dinucleotide interrupt (Scheme A4).

Due to the large residual twist ( $\Delta t = 24.9^\circ$ ) between the nonisosteric G·U and U·G pairs, a high twist (MD =  $39.8^\circ$ , X-ray =  $37.1^\circ$ ) and a low twist (MD =  $25.4^\circ$ , X-ray =  $27.8^\circ$ ) value persists at the tandem UG (Scheme A3) and GU steps (Scheme A4), respectively. Despite very high ( $\Delta t = +24.9^\circ$ ) and very low ( $\Delta t = -24.9^\circ$ ) residual twist at the UG and GU base steps, predicted extreme overwinding and underwinding are moderated and absorbed by local changes in the sugar-phosphate backbone (see Discussion). As expected, the overwinding (MD =  $39.4^\circ$ , X-ray =  $37.5^\circ$ ) and underwinding (MD =  $24^\circ$ , X-ray =  $26.9^\circ$ ) feature is observed (Fig. 3E) at the WC/G·U and G·U/WC base steps (Scheme A5). The helical twist at the GG base step remains unchanged, with an average value (MD =  $30.8^\circ$ , X-ray =  $33.1^\circ$ ), as  $\Delta t$  is  $0^\circ$  between them.

### STRUCTURAL CONTEXT OF G·U AND U·G WOBBLE PAIRS AMONG WC PAIRS

In order to understand the role of wobble base pairs in influencing the immediate helical neighborhood, we systematically examined the occurrence of G·U and U·G wobble pairs and their structural context by analyzing high-resolution crystal structure data. One of the striking features of base-pair nonisostericity-mediated structural effects is the differential base-stacking interaction of wobble G·U with flanking base pairs. A wobble G·U pair stacks better when it precedes a WC pair than when it succeeds it (Mizuno and Sundaralingam 1978). This is a direct consequence of the opposite effects of  $\Delta t$ , wherein underwinding at the 5' G·U/WC 3' step due to  $t - \Delta t$  results in better stacking as compared to a poor stacking interaction at the 5' WC/G·U 3' step due to overwinding mediated by  $t + \Delta t$ . Thus, it is more likely that a wobble G·U pair occurs at the beginning of the helical stem (Table 2A) rather than at the end of the helix (Table 2B). Exactly opposite effects are anticipated for U·G wobble pairs due to reversal in the sign and magnitude of  $\Delta t$ . Hence, loops closed by G·U pairs (stems beginning with G·U pairs) are more stable than those closed by U·G pairs (stems beginning with U·G pairs) (Serra et al. 1993). These factors may explain the high occurrence of G·U and U·G



### SCHEME A

**TABLE 1.** Base-pair nonisostericity matrix for *cis*-WC/WC base pairs

$\begin{matrix} 3 \\ 5 \end{matrix}$	W·C	G·U	U·G	A <sup>+</sup> ·C	C·A <sup>*</sup>	G·A	A·G	U·C	C·U	U <sub>l</sub> ·U <sub>h</sub>	U <sub>h</sub> ·U <sub>l</sub>	C <sup>+</sup> ·C	C·C <sup>+</sup>	A <sub>l</sub> ·A <sub>h</sub>	A <sub>h</sub> ·A <sub>l</sub>
W·C	0.0	+14.0	-11.0	+12.9	-9.9	+7.8	+8.0	-8.3	-8.3	+4.0	-26.9	+6.3	-26.3	+17.0	-3.2
G·U	+0.05	0.0	-24.9	-1.2	-24.1	-5.4	-6.2	-22.1	-22.4	-9.6	-40.6	-7.7	-40.6	+2.6	-17.5
U·G	+0.05	0.0	0.0	+24.2	+1.7	+18.8	+19.1	+3.1	+3.2	+15.5	-15.6	+18.0	-14.6	+28.2	+7.8
A <sup>+</sup> ·C	+0.05	0.0	0.0	0.0	-23.2	-4.3	-4.8	-21.3	-21.6	-8.9	-39.7	-6.9	-39.7	+5.0	-15.2
C·A <sup>*</sup>	+0.05	0.0	0.0	0.0	0.0	+17.9	+18.2	+1.2	+1.7	+13.7	-17.5	+16.2	-16.2	+27.2	+6.9
G·A	-1.0	-1.1	-1.1	-1.1	-1.1	0.0	-0.4	-15.7	-16.2	-3.4	-34.4	-1.2	-34.1	+8.7	-11.3
A·G	-1.0	-1.1	-1.1	-1.1	-1.1	0.0	0.0	-15.6	-16.6	-3.8	-34.9	-1.6	-34.6	+8.9	-11.2
U·C	+1.1	+1.1	+1.1	+1.1	+1.1	+2.2	+2.2	0.0	-0.5	+12.4	-18.7	+15.0	-17.7	+25.0	+5.1
C·U	+1.1	+1.1	+1.1	+1.1	+1.1	+2.2	+2.2	0.0	0.0	+12.2	-19.0	+14.5	-17.8	+25.4	+5.4
U <sub>l</sub> ·U <sub>h</sub>	+1.0	+0.9	+0.9	+0.9	+0.9	+2.0	+2.0	-0.1	-0.1	0.0	-31.2	+2.6	-30.1	+12.7	-7.6
U <sub>h</sub> ·U <sub>l</sub>	+1.0	+0.9	+0.9	+0.9	+0.9	+2.0	+2.0	-0.1	-0.1	0.0	0.0	+33.8	-1.4	+43.6	+23.5
C <sup>+</sup> ·C	+1.0	+0.9	+0.9	+0.9	+0.9	+2.0	+2.0	-0.1	-0.1	0.0	0.0	0.0	-32.2	+10.7	-9.7
C·C <sup>+</sup>	+1.0	+0.9	+0.9	+0.9	+0.9	+2.0	+2.0	-0.1	-0.1	0.0	0.0	0.0	0.0	+43.6	+23.2
A <sub>l</sub> ·A <sub>h</sub>	-1.1	-1.1	-1.1	-1.1	-1.1	0.0	0.0	-2.4	-2.4	-2.2	-2.2	-2.2	-2.2	0.0	-20.3
A <sub>h</sub> ·A <sub>l</sub>	-1.1	-1.1	-1.1	-1.1	-1.1	0.0	0.0	-2.4	-2.4	-2.2	-2.2	-2.2	-2.2	0.0	0.0

Quantification of base pair nonisostericity in terms of residual twist ( $\Delta t$ , blue) and radial difference ( $\Delta r$ , red) between WC and nWC pairs and between different nWC base pairs. Base steps with high and low residual twist and radial difference are highlighted in light blue and light red, respectively. Subset of the matrix depicting nonisostericity measure between WC and wobble pairs is enclosed by thick lines. The matrix is symmetric along the principal diagonal with opposite signs.

wobble pairs at the beginning and end of helical stems, respectively, as also seen in ribosomal secondary structures (van Knippenberg et al. 1990; Gautheret et al. 1995; Szymański et al. 2000).

A large number of G·U and U·G wobble pairs flanked by WC and nWC base pairs are also found within the helix (Table 3). These are predominantly flanked by WC base pairs (62.6%). Among those that precede a G·U pair, a large number are purine-pyrimidine base pairs (31.1%), compared to the pyrimidine-purine type (18.8%). Although it is shown above that the  $+\Delta t$  mediated-overwinding brings forth intra-strand destacking, the degree of destacking is much lower when a purine-pyrimidine base pair precedes a G·U wobble than a pyrimidine-purine base pair (Gautheret et al. 1995). This is consistent with the thermodynamic studies on the near-neighbor effects, which indicate that G·U pairs preceded by a G·C base pair are more stable (He et al. 1991), thus ac-

counting for their large occurrence (23.0%) compared to A·U base pairs (8.1%).

On the other hand, among WC pairs that succeed a G·U wobble, pyrimidine-purine pairs occur more frequently (28.9%) than purine-pyrimidine base pairs (21.0%). A C·G base pair succeeding a G·U wobble is found to be thermodynamically more stable (He et al. 1991) and hence occurs in high frequency (22.7%) than G·C (14.0%), A·U (7.0%), and U·A base pairs (6.1%).

### STRUCTURAL CONTEXT OF WOBBLE PAIRS AMONG nWC PAIRS

Interestingly, nWC pairs flanking wobble G·U base pairs exhibit strong positional preferences (Table 3). A large number of them (31.5%) are found either preceding G·U or succeeding U·G pairs. On the other hand, occurrence of



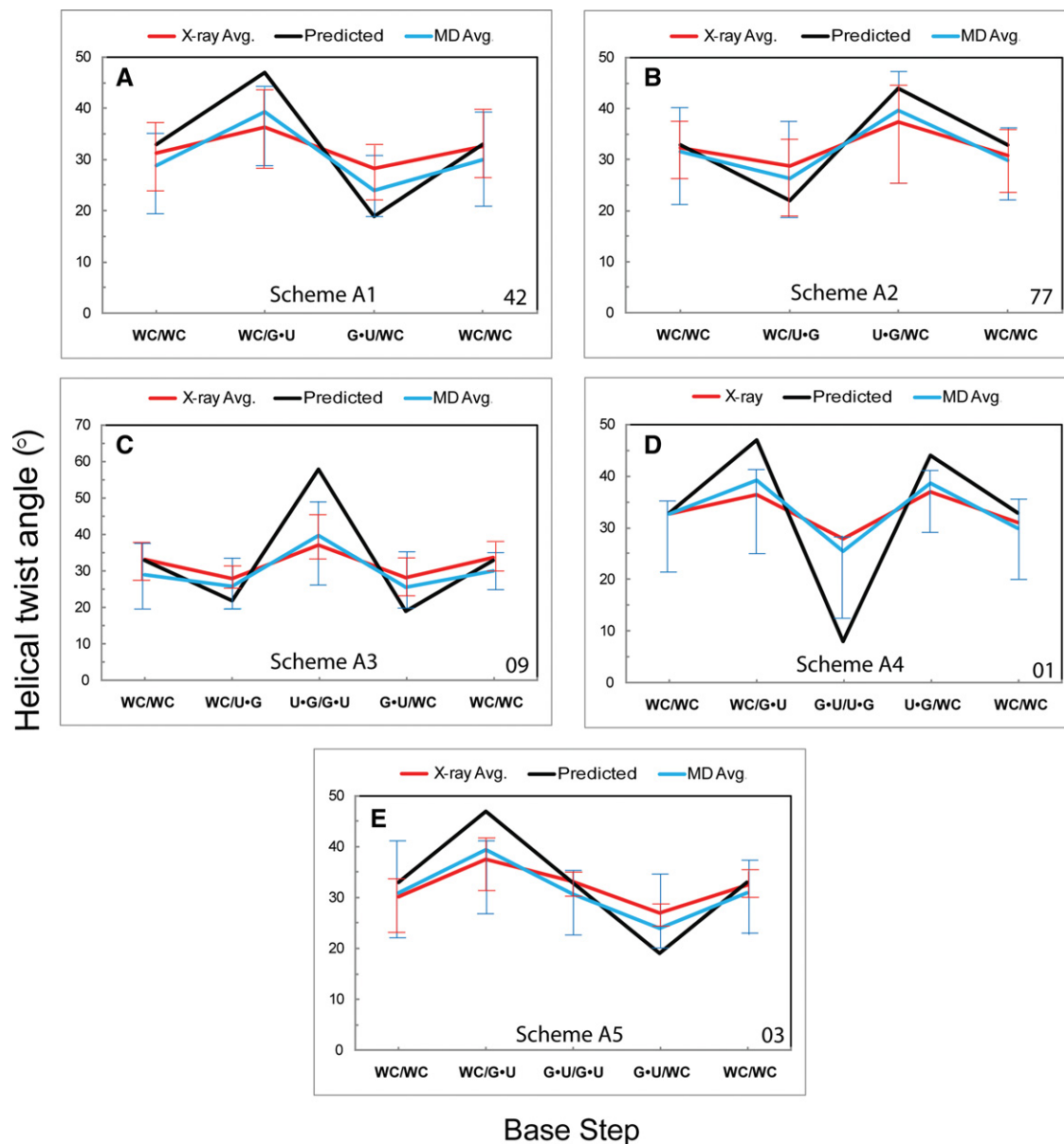


**FIGURE 3.** Comparison of helical twist angles in RNA duplexes interrupted by wobble pairs. Average values of helical twist angles at different base steps in RNA duplexes interrupted by (A) G-U pair (Scheme A1), (B) U-G pair (Scheme A2), (C) U-G pair followed by G-U pair (Scheme A3), (D) G-U pair followed by U-G pair (Scheme A4), and (E) two G-U pairs (Scheme A5). Twist angles based on residual twist ( $\Delta t$ ) (black), MD simulations (blue), and crystal structure data (red) are shown. Differences between the predicted and the observed helical twist angle at WC/wobble or wobble/WC steps may be due to compensatory adjustments in the sugar-phosphate backbone conformations to minimize the effect of residual twist. Numbers at the bottom right of each panel denote the number of instances in X-ray structures found and considered for comparison.

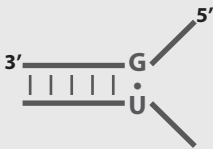
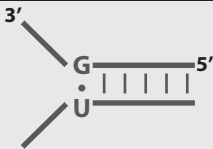
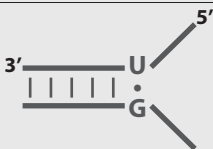
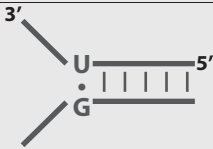
nWC pairs succeeding G-U or preceding U-G are rather less (5.8%) (Table 3). Preference for a specific nWC base pair is dictated by its ability to provide better stacking with the wobble base pair.

#### A-G pair preceding G-U

Among the preceding nWC pairs, an A-G pair is more frequent (34.6%) followed by U-G and G-U base pairs, similar to the trend observed in ribosomal RNA secondary structures

(Gautheret et al. 1995). A-G base pairs preceding a G-U wobble are mostly involved in a *trans*-Hoogsteen/Sugar Edge (*trans*-H/SE) base-pairing scheme (Leontis et al. 2002), involving N7(A) ... N2(G), N6(A) ... N3(G), and N6(A) ... O2'(G) hydrogen bonds. This scheme entails nonisostericity to the extent of  $\Delta r = +0.4 \text{ \AA}$  and  $\Delta t = -30.9^\circ$  (Table 4; Fig. 4F), warranting local underwinding concomitant with enhanced intra-strand base stacking with the wobble G-U pair (Fig. 5A). Incidentally *trans*-H/SE A-G pairs are the most stable members of the *trans*-H/SE base-pair family (Mládek

TABLE 2. Frequency of terminal wobble pairs

	Helical schemes	Total number of instances
A		13
B		05
C		02
D		29

G·U and U·G pairs are frequently found at the beginning and at the end of the helix, respectively.

et al. 2009) and are observed in kink-turn motifs (Klein et al. 2001), GNRA tetraloops (Jucker et al. 1996), sarcin/ricin loops (Szewczak et al. 1993; Correll et al. 1999), and E-loops (Wimberly et al. 1993). Thermodynamics of loop formation indicate loops with tandem *trans*-H/SE A·G pairs preceding a G·U wobble are more stable (Walter et al. 1994). However, G·A base pairs with the same hydrogen bonding scheme

are rarely observed preceding a G·U wobble, occurring at just two sites (1.1%). It may be noted that this base-pairing scheme renders the G·A pair to be non-self-isosteric and subtends a high value of residual twist ( $\Delta t = +59.5^\circ$ ) and  $\Delta r = +0.4 \text{ \AA}$  with the succeeding G·U pair (Fig. 4G), causing significant overwinding and poor inter-strand base stacking (Fig. 5B), thus accounting for their rare occurrence.

### U·G pair preceding G·U

A U·G wobble is the second most frequently observed nWC pair preceding a G·U wobble (21.7%) and is also the most abundant among tandem wobble motifs (Gautheret et al. 1995; Masquida and Westhof 2000). Despite a large  $\Delta t$  ( $+24.9^\circ$ ) with the succeeding G·U wobble (Fig. 4C), high occurrences of this motif are attributed to its thermodynamic stability (Wu et al. 1995) due to strong inter-strand stacking (between the guanines) and  $-\Delta t$  ( $-11.0^\circ$  and  $-14.0^\circ$ )-mediated enhanced intra-strand stacking with the flanking WC pairs (Biswas et al. 1997; Deng and Sundaralingam 2000).

### G·U pair preceding G·U

Two successive G·U base pairs are the next most frequently observed (18.9%) amid WC paired RNA duplex. Isostericity of base pairs ( $\Delta t = 0^\circ$ ) at the tandem interface maintains an average helical twist angle of  $33^\circ$ , causing intermediate base-stacking interactions (Masquida and Westhof 2000). However, compared to the previous case, this motif exhibits diminished stacking with the flanking WC pairs owing to a high ( $+14.0^\circ$ ) and low  $\Delta t$  ( $-14.0^\circ$ ) with the preceding and succeeding WC base pairs (Fig. 4E). Also, thermodynamic studies have shown that duplexes comprising successive G·U pairs are less stable compared to those with the U·G/G·U motif (He et al. 1991) and, therefore, less frequently observed. MD simulations of miniduplexes comprising

TABLE 3. Frequency and structural context of intra-helical wobble pairs and their flanking base pairs

Total no. of occurrences of G·U	Frequency of flanking WC base pairs 5' WC/G·U/WC 3'	Frequency of preceding nWC base pairs 5' nWC/G·U/WC 3'	Frequency of succeeding nWC base pairs 5' WC/G·U/nWC 3'
568 (100%)	356 (62.67%)	179 (31.51%)	33 (5.80%)
	GC/G·U/WC 82 (23.03%)	A·G/G·U/WC 62 (34.63%)	WC/G·U/A·G 09 (27.27%)
	CG/G·U/WC 44 (12.35%)	U·G/G·U/WC 39 (21.78%)	WC/G·U/G·A 09 (27.27%)
	AU/G·U/WC 29 (8.14%)	G·U/G·U/WC 34 (18.99%)	WC/G·U/U·G 05 (15.15%)
	UA/G·U/WC 23 (6.46%)	A·C/G·U/WC 13 (7.26%)	WC/G·U/A·C 03 (9.09%)
	WC/G·U/CG 81 (22.75%)	C·U/G·U/WC 12 (6.70%)	WC/G·U/U·U 03 (9.09%)
	WC/G·U/GC 50 (14.04%)	U·U/G·U/WC 07 (3.91%)	WC/G·U/C·A 02 (6.06%)
	WC/G·U/AU 25 (7.02%)	G·G/G·U/WC 05 (2.79%)	WC/G·U/A·A 02 (6.06%)
	WC/G·U/UA 22 (6.17%)	A·A/G·U/WC 05 (2.79%)	
		G·A/G·U/WC 02 (1.11%)	

Occurrences of nWC pairs preceding wobble G·U are comparatively more than those that succeed it. Note 5' nWC/G·U 3' is equivalent to 5' U·G/nWC 3'.

TABLE 4. Base-pair nonisosteric matrix for *trans*-H/SE base pairs

3' 5'	WC	G·U	U·G	<i>t</i> -H/SE A·U	<i>t</i> -H/SE U·A	<i>t</i> -H/SE A·C	<i>t</i> -H/SE C·A	<i>t</i> -H/SE A·G	<i>t</i> -H/SE G·A*	<i>t</i> -H/SE U·G	<i>t</i> -H/SE G·U*	<i>t</i> -H/SE C·U	<i>t</i> -H/SE U·C*	<i>t</i> -H/SE C·C	<i>t</i> -H/SE A·A	<i>t</i> -H/SE G·G
WC	0.0	+14.0	-11.0	+47.2	+38.9	+50.6	+48.5	+44.8	-45.6	+46.1	-44.5	+52.3	-53.8	+49.7	+51.2	+17.0
G·U	+0.05	0.0	-24.9	+33.2	+24.9	+36.7	+32.4	+30.9	-59.5	+32.1	-58.5	+38.3	-67.8	+35.7	+37.3	+4.1
U·G	+0.05	0.0	0.0	+58.7	+50.2	+62.5	+59.8	+56.7	-34.4	+30.7	-33.4	+63.3	-42.9	+61.8	+63.2	+29.2
<i>t</i> -H/SE A·U	+0.5	+0.4	+0.4	0.0	-8.8	+3.4	+0.7	-2.3	-92.8	-1.7	-91.6	+4.5	-101.6	+1.9	+4.0	-29.2
<i>t</i> -H/SE U·A	-0.3	-0.3	-0.3	-0.8	0.0	-12.3	+11.8	+6.5	-84.3	+7.5	-83.3	+14.2	-92.7	+11.6	+12.9	-20.7
<i>t</i> -H/SE A·C	+0.5	+0.4	+0.4	0.0	+0.8	0.0	-2.7	-5.8	-96.2	-5.1	-95.1	+1.2	-105.0	-1.4	+0.8	-32.6
<i>t</i> -H/SE C·A	+0.7	+0.6	+0.6	+0.2	+1.0	+0.2	0.0	-3.1	-93.9	-3.1	-92.9	+3.9	-103.1	+1.2	+3.3	-30.3
<i>t</i> -H/SE A·G	+0.5	+0.4	+0.4	0.0	+0.8	0.0	-0.2	0.0	-90.4	+1.1	-89.3	+6.9	-99.2	+4.3	+6.4	-26.8
<i>t</i> -H/SE G·A*	+0.5	+0.4	+0.4	0.0	+0.8	0.0	-0.2	0.0	0.0	+91.6	+1.3	+97.8	-8.6	+95.2	+96.9	+63.6
<i>t</i> -H/SE U·G	-0.3	-0.3	-0.3	-0.8	0.0	-0.8	-0.9	-0.8	-0.8	0.0	-90.5	+6.2	-100.0	+3.1	+5.7	-28.0
<i>t</i> -H/SE G·U*	-0.3	-0.3	-0.3	-0.8	0.0	-0.8	-0.9	-0.8	-0.8	0.0	0.0	+96.7	-9.4	+94.1	+95.7	+62.5
<i>t</i> -H/SE C·U	+0.6	+0.5	+0.5	+0.1	+0.9	+0.1	0.0	+0.3	+0.3	+0.9	+0.9	0.0	-107.0	-2.6	-1.0	-34.1
<i>t</i> -H/SE U·C*	+0.6	+0.5	+0.5	+0.1	+0.9	+0.1	0.0	+0.3	+0.3	+0.9	+0.9	0.0	0.0	+104.4	+105.7	+72.0
<i>t</i> -H/SE C·C	+0.6	+0.5	+0.5	+0.1	+0.9	+0.1	-0.1	+0.1	+0.1	+0.9	+0.9	0.0	0.0	0.0	+2.1	-31.5
<i>t</i> -H/SE A·A	+0.6	+0.6	+0.6	+0.1	+0.9	+0.1	0.0	+0.1	+0.1	+0.9	+0.9	0.0	0.0	0.0	0.0	-33.2
<i>t</i> -H/SE G·G	+0.5	+0.5	+0.5	0.0	+0.8	0.0	-0.1	0.0	0.0	+0.8	+0.8	-0.1	-0.1	0.0	-0.1	0.0

Comparison of residual twists ( $\Delta t$ , green) and radial differences ( $\Delta r$ , brown) of *trans*-H/SE nWC pairs with WC, *cis*-G·U, and *cis*-U·G base pairs (gray). Base steps with low residual twist are highlighted in light green. Note that not all base-pair combinations of this family are feasible. G·A\*, G·U\*, and U·C\* represent *trans*-H/SE A·G, U·G, and C·U base pairs, respectively, but in flipped orientation. Glycosidic bond angles and C1' ... C1' separations are as suggested by Leontis et al. (2002). The matrix is symmetric along the principal diagonal with opposite signs.

consecutive G·U base pairs of four or more in a WC duplex suggest that loss of hydrogen bonds leads to a less stable nature of such duplexes (data not shown).

### A·G pair succeeding G·U

Among the succeeding nWC pairs, A·G pairs occur frequently (27.2%). It is observed that the succeeding A·G base pairs in nearly every situation are paired in the *cis*-WC/WC scheme (Fig. 5C). A *cis*-WC/WC A·G base-pairing scheme at this step promotes better stacking (Fig. 5C) due to the low  $\Delta t$  ( $-6.2^\circ$ )-mediated underwinding (Fig. 4H), compared to the large  $\Delta t$  ( $+30.9^\circ$ )-mediated poor stacking interactions of a *trans*-H/SE scheme. Thus, the observed base-pairing schemes for the preceding and succeeding A·G pairs (Fig. 5A,C) induce negative  $\Delta t$  with the wobble G·U pair enhancing base stacking

and stability, providing a rationale for the observed juxtapositions of A·G and G·U wobble pairs.

### G·A pair succeeding G·U

G·A pairs succeeding a G·U wobble pair are equally observed (27.2%). G·A pairs, like A·G pairs, exhibit variations in base-pairing schemes. It is seen that succeeding G·A pairs within the helical stem are paired via a *cis*-WC/WC scheme, while those at the helical termini closing loops are paired in a *trans*-H/SE scheme.

*cis*-WC/WC G·A pairs are accommodated within the helix without causing significant changes to the duplex structure (Leonard et al. 1994). It promotes better intra-strand base stacking with the preceding wobble G·U (Fig. 5D) due to the low  $\Delta t$  ( $-5.4^\circ$ )-mediated underwinding (Fig. 4I).

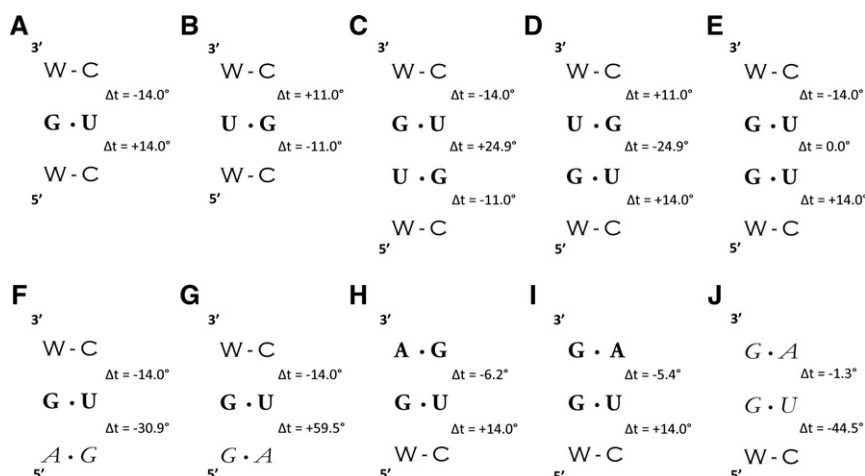


**FIGURE 4.** Structural context of  $\Delta t$ . Predicted residual twist angle between various base-pair steps (A–J).  $+\Delta t$  suggests overwinding, accompanied almost always by diminished intra-strand stacking and vice versa. nWC base pairs paired via *trans*-H/SE are italicized.

On the other hand, presence of *trans*-H/SE pairs within the helical region are expected to significantly alter the regular backbone geometry (Baeyens et al. 1996) and hence would be preferred at helical breakpoints or at helical termini closing loops, wherein such G·A pairs, predominantly, stack well (Burkard et al. 1999). Most interestingly, G·U wobble pairs preceding such G·A pairs assume a hydrogen bonding scheme similar to a *trans*-H/SE U·G pair (Leontis et al. 2002), with a single hydrogen bond between N2(G) ... O4(U) concomitant with a larger C1' ... C1' separation (11.2 Å). The resulting G·U wobble subtends a low  $\Delta t$  ( $-1.3^\circ$ ) with the succeeding G·A (Fig. 4J) enhancing intra-strand base-stacking interactions (Fig. 5E).

### U·G pair succeeding G·U

A U·G wobble pair succeeding a G·U pair is less frequently observed (15.1%). The G·U/U·G motif is less preferred due to unfavorable steric contacts within it and the sugar-phosphate backbone which may severely influence the regular A duplex geometry (Gautheret et al. 1995). As discussed earlier, a negative  $\Delta t$  ( $-24.9^\circ$ ) at this base step promotes better intra-strand base stacking. However, a positive  $\Delta t$  ( $14^\circ$  and  $11^\circ$ ) prevails between a WC pair preceding and succeeding wobble G·U and U·G pairs, respectively (Fig. 4D). As reiterated several times in this article, they induce overwinding, causing poor inter-strand stacking interactions with the flanking WC base pairs (Biswas and Sundaralingam 1997). The G·U/U·G motif thus exposes the overwound destacked

faces toward the helix (Gautheret et al. 1995) and, as such, has the lowest thermodynamic stability (He et al. 1991), explaining the extremely low occurrence of this motif.

Apart from the above-discussed nWC base pairs, A·C, C·U, U·U, A·A, G·G and A·C, U·U, C·A, A·A are the other nWC pairs found preceding or succeeding G·U wobble pairs, respectively. They occur in fewer numbers and do not show any regular pattern.

### G·U AND U·G WOBBLE PAIRS IN PROTEIN-RNA INTERACTIONS

Base-pair geometry of wobble pairs creates unique features on the structure and electrostatic surface potential landscape of the duplex, offering itself for metal ion binding and protein recognition interactions. The local electrostatics of the major groove are altered when the free carbonyl group of uracil (O4) replaces the invariant amino group of G·C (N4) or A·U (N6) WC pairs, thus causing localized regions of deep negative electrostatic potential (Varani and McClain 2000; Xu et al. 2007). The metal ion binding at these sites is an important requirement for substrate recognition by group I intron ribozymes (Allain and Varani 1995). Although the localized negative electrostatic surface potential at the deep major groove allows binding of metal ions or water, its narrow groove width could

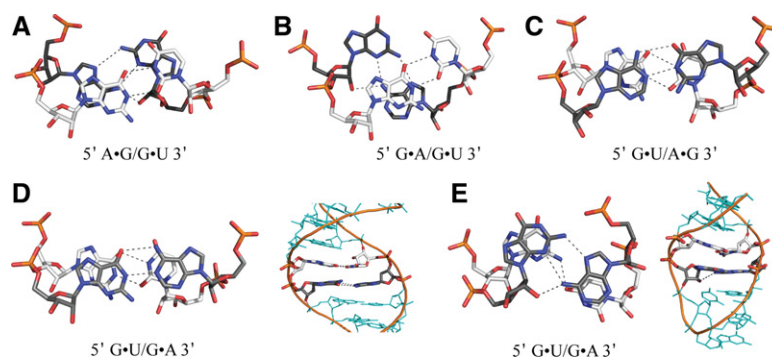


**FIGURE 5.** Nature of stacking interactions at the interface of wobble G·U and G·A base pairs. Stacking of nWC G·A and A·G base pairs with wobble G·U in different structural and hydrogen bonding contexts. Carbon atoms of A·G and G·A base pairs are colored gray, while those of G·U pairs are colored white. (A) A *trans*-H/SE A·G pair preceding G·U wobble exhibits better intra-strand base stacking due to low  $\Delta t$  ( $-30.8^\circ$ ). (B) G·A pair preceding G·U wobble results in inter-strand base stacking due to large  $\Delta t$  ( $+59.5^\circ$ )-mediated overwinding. (C) A *cis*-WC/WC A·G base pair succeeding a G·U wobble manifests in better intra-strand base stacking due to low  $\Delta t$  ( $-6.2^\circ$ ). (D) A *cis*-WC/WC G·A pair succeeding a G·U wobble and occurring within the helical stem (right panel) (pdb: 1fjg). (E) G·A paired in *trans*-H/SE scheme and occurring at the helical termini (right panel) (pdb: 1fjg). Both these pairing schemes facilitate good intra-strand stacking as a result of low  $\Delta t$  ( $-5.4^\circ$  and  $-1.3^\circ$ ) subtended with the succeeding G·U wobble.



hinder interactions with proteins. Hence, most protein-RNA interactions are confined along the minor groove (Hermann and Westhof 1999).

### Protein contacts are mediated by the exocyclic N2 amino group of wobble G·U

Any feature that breaks the monotony of the direct read-out of WC pairs along its minor groove side could serve as a unique site for recognition interaction. Occurrence of a nWC pair amid WC pairs alters the local geometry of the duplex and presents distinctive donor/acceptor groups for interactions. Presence of nWC pairs such as a G·U or U·G wobble not only influence the minor groove surface, due to  $\Delta t$ -mediated mechanistic effects but also exposes the unpaired exocyclic amino group. The significance of these wobble pairs is underscored by their involvement in a large number of protein-RNA interactions.

A G·U wobble pair in the acceptor stem of *Escherichia coli* tRNA<sup>Ala</sup> (Hou and Schimmel 1988; McClain and Foss 1988) and in the D stem of yeast tRNA<sup>Asp</sup> (Pütz et al. 1991) is found to be crucial for recognition and aminoacylation by their cognate synthetases. Similarly a conserved G·U wobble pair is an important requirement for splicing activity of ribozymes (Peebles et al. 1995; Strobel and Cech 1995). Replacement of a G·U wobble by a nonisosteric G·C or U·G pair retains the N2 functional group, but such nonisosteric substitutions, nevertheless, impede recognition and aminoacylation of tRNA<sup>Ala</sup> (Hou and Schimmel 1988; Park et al. 1989). On the other hand, substitution of base pairs isosteric to the G·U wobble, such as A·C and I·U, which lack the N2 exocyclic amino group, is shown to result in comparatively weaker interactions at the catalytic core of *Tetrahymena* ribozyme (Strobel and Cech 1995). However, base-pair substitutions which are both isosteric and comprise the N2 amino group restore the catalytic activity (Strobel and Cech 1995), suggesting the role of both base-pair isostericity and the determinant functional group in interaction and catalysis.

Protein-RNA interactions involving the wobble base pairs, G·U and U·G, are, by and large, mediated by hydrogen bond interactions between the exocyclic N2 amino group and side chains of Gln, Asp, Glu, Asn, and His. These interactions generally arise from the helical regions of protein (helix-loop-helix/ $\beta$ - $\alpha$ - $\beta$  motifs) and reside along the minor groove of the RNA duplex. G·U and U·G wobble pairs present within the helical stems as well as at the termini participate equally. Although a majority of these minor groove interactions engage the N2 amino group, a few instances involving N3, O2, and 2'-OH are also found. Likewise, interactions involving peptide carbonyl groups are seen occasionally.

An example of such interaction with N3 (G) is observed in the 50S ribosomal subunit of *E. coli* (pdb: 3r8s). The loop region of ribosomal protein L18 positioned along the minor groove side of the G<sub>9</sub>·U<sub>111</sub> wobble facilitates hydrogen bond interactions with Ser45 (O $\gamma$ ) and G9 (N3). Gly44, adjacent

to the interacting serine, forms a hydrogen bond involving peptide carbonyl with 2'-OH of G9. Ser214 from the *Haloarcula marismortui* large ribosomal protein L2P (pdb: 1s72) also participates in a similar main chain hydrogen-bonded interaction with 2'-OH of G<sub>1898</sub> which pairs with U<sub>1939</sub>. A rare protein-nucleic acid interaction involving methionine is observed in the *H. marismortui* large ribosomal subunit (pdb: 1s72). Met23 of the L30P subunit interacts with U<sub>942</sub>·G<sub>1024</sub> of 23S rRNA through main-chain and side-chain groups. Flipping of the unpaired A<sub>943</sub> succeeding the U<sub>942</sub>·G<sub>1024</sub> pair positions Met23 into the minor groove, facilitating the main-chain carbonyl and S $\delta$  in forming hydrogen bonds with 2'-OH (G<sub>1024</sub>) and N2, respectively.

G·U wobble pairs accommodate eight conserved hydration sites, five at the major groove and three at the minor groove (Auffinger and Westhof 1998). Among them, three (two major groove and one minor groove) hydration sites were proposed as integral elements of the tRNA<sup>Ala</sup> acceptor stem and implicated in synthetase-tRNA interaction (Mueller et al. 1999). The invariant water molecule at the minor groove that forms a hydrogen bond network bridging N2 (G), O2 (U), and 2'-OH (U) atoms of the wobble pair is displaced upon protein-mediated interaction with the G<sub>38</sub>·U<sub>453</sub> wobble pair in the *Deinococcus radiodurans* large ribosomal subunit (pdb: 2zjr). Here, Arg40 of the ribosomal protein L4 interacts with G<sub>38</sub>·U<sub>453</sub> of 23S rRNA by forming hydrogen bonds between NH1, NH2 (Arg40), and O2 (U<sub>453</sub>) (Fig. 6A).

### Wobble pair-mediated kink in $\alpha$ helix

Interactions of RNA with proteins or RNA are known to bring about conformational changes both in protein and RNA (Frankel and Smith 1998; Ellis and Jones 2008). Instances of conformational change in proteins, seemingly influenced by wobble pairs, are noticed in the large subunit of bacterial ribosomes. A distinct bend ( $\sim 25^\circ$ ) is observed in helix 3 of *E. coli* 50S ribosomal protein L20 interacting with 23S rRNA (pdb: 3r8s). Interestingly, such a bend of nearly the same magnitude is also found in the ribosomal protein of *Thermus thermophilus* (pdb: 2wdl) and *D. radiodurans* (pdb: 2zjr). The site of the bend, in all of these, entices a number of interactions (Fig. 6E) linking the wobble pairs of the RNA duplex and the protein. The tandem wobble pairs U<sub>534</sub>·G<sub>559</sub>/G<sub>535</sub>·U<sub>558</sub> of the *E. coli* 23S rRNA interact with Asp48, Gln51, and Gln55 along the minor groove face of the RNA duplex. Asp48 and Gln51 form hydrogen bond interactions with N2 amino and O2' hydroxyl groups of the U<sub>534</sub>·G<sub>559</sub> wobble, while Gln55 makes contact with the N2 amino group of the succeeding G<sub>535</sub>·U<sub>558</sub> wobble. Apart from hydrogen bond interactions with the wobble pairs, Gln51 and Gln55 are engaged in side chain-side chain interactions. A conserved basic residue Arg52 arising from the same helix makes multiple hydrogen bond interactions with the phosphate backbone atoms of the wobble G<sub>535</sub>·U<sub>558</sub> and the succeeding WC pair.

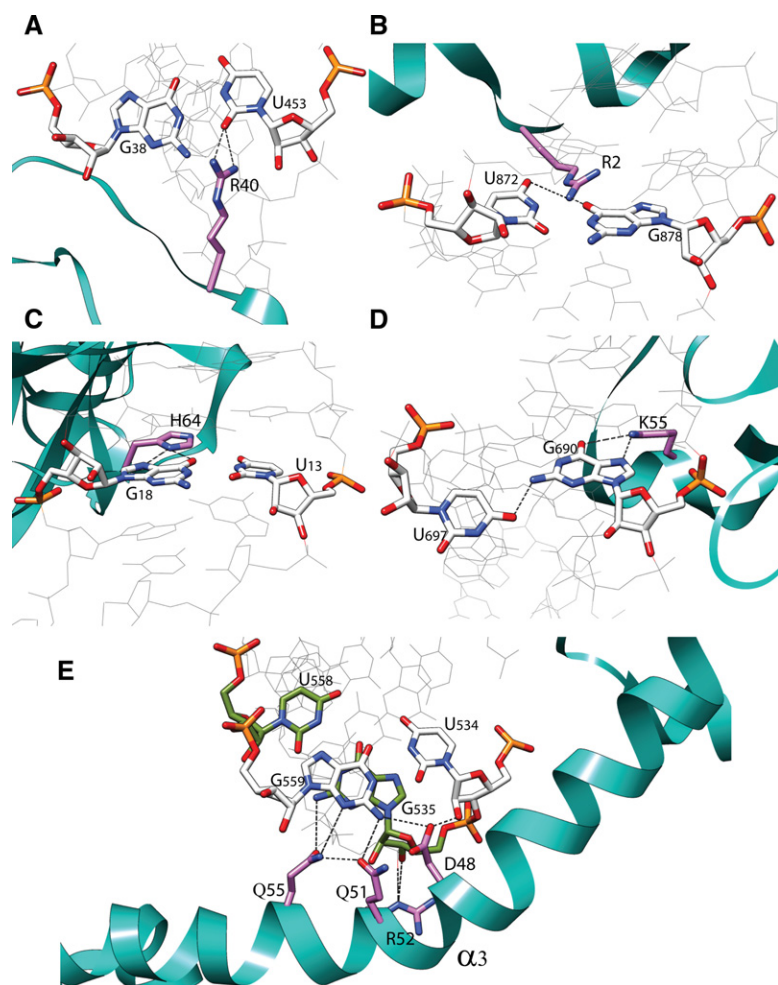


**FIGURE 6.** G-U wobble pair-mediated protein-RNA interactions. (A) Interaction between arginine of L4 protein and O2-carbonyl (U<sub>453</sub>) of wobble G<sub>38</sub>·U<sub>453</sub> of *Deinococcus radiodurans* 23S rRNA along the minor groove. Interaction along the major groove involving (B) Arg2 from the *Haloarcula marismortui* ribosomal protein L2P and the U<sub>872</sub>·G<sub>878</sub> wobble pair of 23S rRNA, (C) His64 from the mouse NF-κB p50 subunit and the U<sub>13</sub>·G<sub>18</sub> wobble pair, (D) Lys55 from the *Thermus thermophilus* ribosomal protein S11 and the G<sub>690</sub>·U<sub>697</sub> wobble pair of 16S rRNA. (E) Extensive hydrogen bond interactions between polar residues of the *Escherichia coli* L20 ribosomal protein with tandem U<sub>534</sub>·G<sub>559</sub>/G<sub>535</sub>·U<sub>558</sub> pairs of 23S rRNA. Note the sharp bend in helix α3 at the interaction loci involving wobble pairs.

### Wobble-mediated interactions at the major groove

Although the narrow nature of major groove width of RNA duplexes limits its interaction with proteins, uncoupling of helices at large internal loops (Weeks and Crothers 1993), together with groove width variations, due to the occurrence of nWC base pairs (Hermann and Westhof 1999), facilitates its accessibility for protein recognition interaction. Presence of potential hydrogen bond acceptors O6, N7, and O4 along the major groove of the wobble pair suggests interactions mostly involving positively charged amino acid residues. A few such instances of major groove interactions involving G-U wobble pairs are observed, primarily mediated through hydrogen bonds with Arg, His, and Lys.

The *H. marismortui* large ribosomal protein L2P (pdb: 1s72) provides an example of the major groove interaction involving both O6 and O4 acceptors. Helical uncoupling at the loop in 23S rRNA exposes the terminal U<sub>872</sub>·G<sub>878</sub> wobble pair for interaction with Arg2 of ribosomal protein L2P. The succeeding G<sub>873</sub>·A<sub>876</sub> pair and the flipped out G<sub>877</sub> facilitates Arg2 to access the wobble pair through the major groove and forms hydrogen bonds with NH<sub>2</sub> ... U<sub>872</sub> (O4) and G<sub>878</sub> (O6) (Fig. 6B). The mouse nuclear factor NF-κB p50 subunit (pdb: 1ooa) recognizes the distorted major groove surface of the RNA aptamer and makes conserved interactions with the U<sub>13</sub>·G<sub>18</sub> wobble pair (Huang et al. 2003). His64 (ND1) from the L1 loop region of NF-κB p50 subunit interacts with G<sub>18</sub> (N7 and O6) in ways identical to the contacts (Fig. 6C) made with its DNA substrate (Huang et al. 2003). Interactions involving a noncanonical G-U base pair at the major groove interaction site is observed in the *T. thermophilus* 16S rRNA (pdb: 1fjg). A stretched G<sub>690</sub>·U<sub>697</sub> pair (*trans*-H/SE U-G) with the C1' ... C1' separation of 11.4 Å and a single hydrogen bond (N2-H ... O4) interacts with Lys55 of ribosomal protein S11 involving N7 and O6 of G<sub>690</sub> (Fig. 6D).

Analyses indicate that Δ*t*-induced local helical twist variations are not altered even when wobble pairs are involved in interaction with proteins. Analyses of C1' ... C1' distance and helical twist angles show minor changes in the helical twist angles (±2°) and C1' ... C1' distances (−0.15 Å).

### G-U WOBBLE IN LONG-RANGE INTERACTIONS

Apart from their role as potential sites for protein binding, nWC pairs play a role in the compact folding of large molecules such as ribosomes (Nissen et al. 2001). They participate in packing of helices through long-range interactions in motifs such as kink-turn (Klein et al. 2001), along-groove packing (Gagnon and Steinberg 2002), and the A-wedge motif (Gagnon and Steinberg 2010).

G-U wobble-mediated tertiary interactions are of critical importance in the “along-groove packing motif” (Gagnon and Steinberg 2002). Here, a “central” G-U wobble pair is engaged in long-range interactions with a WC base pair along the interface formed by the minor grooves of the two interacting

helices. The nonisosteric nature of the G·U pair compared to a WC pair causes U of the G·U pair to move away (due to residual twist) from the minor groove, creating enough room to facilitate close interaction with the WC pair (G·C) of the other helix (Gagnon et al. 2006). This promotes tight packing of the two helices mediated by hydrogen bond interactions (Gagnon and Steinberg 2002; Gagnon et al. 2010), as shown in Figure 7A. Mutation of the G·U wobble to WC or to other nWC pairs proves detrimental for helical packing, resulting in ribosomal inefficiency (Gagnon et al. 2006). Replacement of G·U by a U·G pair would not only alter the minor groove surface complementarity ( $G\cdot U \neq U\cdot G$ ) but also lead to steric clashes at the interface (Gagnon et al. 2010), weakening the helical packing. Likewise, helical packing would be destabilized when the groove packing motif comprises two central WC base pairs (Gagnon and Steinberg 2002). Replacement of G·U wobble by G·C results in a significant change in the orientation of ribose sugars of the “internal” bases, leading to a loss in minor groove interactions (Gagnon et al. 2010). Also, differences in base-pair geometry of G·C compared to wobble G·U results in the loss of hydrogen bond interactions of the N2 amino group with the ribose sugar of the base of the facing helix, creating an opening or “crack” (Fig. 7B) at the interface (Gagnon et al. 2006, 2010). It is further observed that preference for G·C or C·G as “central” pairs over A·U or U·A (Gagnon et al. 2006) reflects the need for maximizing long-range interactions for packing stability, provided by additional interaction involving the exocyclic N2 amino group of guanine vis-a-vis adenine. However, swapping of G·U and WC

pairs of the two interacting helices does not affect helical packing, due to the complementary nature of the interaction (Gagnon et al. 2006). The critical nature of the presence of the G·U wobble pair in defining the interactions responsible for “along-groove packing motif” is evident.

## DISCUSSION

Nucleic acids owe their remarkable structures to the underlying geometries of their constituent base pairs. The unique WC base-pairing scheme endows DNA with both sense and structural complementarity, imperative for structural uniformity and faithful replication. Besides the geometrical equivalence (isostericity) of WC pairs, the nearly identical glycosidic bond angles allow interchangeability of bases within them. These render WC pairs to be not only isosteric but also self-isosteric, facilitating substitution of any one of the four base pairs (A·T, G·C, T·A, and C·G) in a duplex without significantly altering the duplex structure. Other possible base pairs which do not conform to these are said to be nonisosteric with WC pairs. Such nonisosteric base pairs are found in fairly large numbers in RNA, although WC pairs dominate the arena, underscoring the profound importance of base-pair isostericity and base-pair self-isostericity in governing the structure and function of nucleic acids in general. It is, therefore, of utmost importance to understand and obtain an estimate of the degree of nonisostericity of nWC base pairs compared to the preponderant WC pairs. It is recognized that the presence of nWC pairs amid WC pairs influences the structure of nucleic acid duplexes, and nonequivalent base-pair substitutions are found to eliminate function (Chang et al. 1999; Zhong et al. 2006), thus playing a major role in the evolution of macromolecules (Gutell et al. 1994). However, rationale for the observed nWC base pair-mediated mechanistic effects in RNA duplexes still remains vague. In this context, we have attempted to define and quantify base-pair nonisostericity between any two base pairs (WC/WC or WC/nWC or nWC/nWC) by means of a simple and discernible metric ( $\Delta t$  and  $\Delta r$ ) that also enables visualization of their mechanistic effects in a straightforward manner.

Utility of such a metric is illustrated by taking the example of the wobble G·U, which has attracted considerable attention due to its abundance and implications in biological functions. Its juxtaposition with a WC pair imparts an intrinsic residual twist ( $\Delta t$ ) of  $14^\circ$  even in the absence of the prescribed helical twist of  $33^\circ$ . Its influence on the helical twist angles is manifested as local helical overwinding and underwinding, depending on whether the wobble G·U succeeds ( $+\Delta t$ ) or precedes ( $-\Delta t$ ) a WC pair, respectively. This observation is consistent with X-ray crystal structure and MD simulation data. Origin of such observations seen in RNA duplexes interrupted by a U·G pair, as well as GU and UG dinucleotides, can be readily linked to the effect of magnitude and sign of  $\Delta t$ .

It is seen that an insertion of a G·U wobble (or any nWC pair) amid a RNA duplex comprising WC base pairs creates

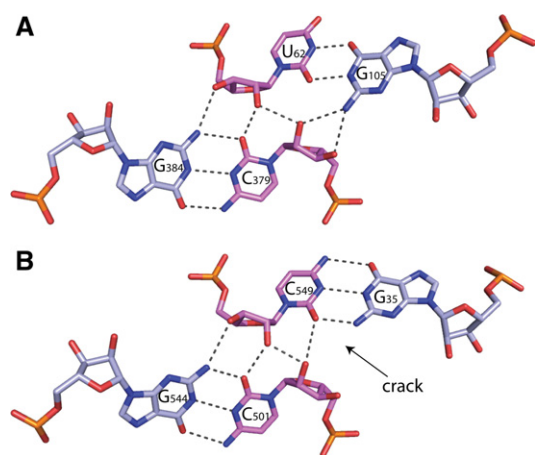


**FIGURE 7.** G·U wobble in long-range interactions. Along-groove packing in RNA mediated through extensive hydrogen bond interactions involving internal (pink) and external (blue) base pairs of the participating helices along the minor groove. (A) Interactions involving U<sub>62</sub>·G<sub>105</sub> and G<sub>384</sub>·C<sub>379</sub> base pairs of *T. thermophilus* 16S rRNA (pdb: 1fjg). Presence of a wobble pair leads to a complementary fit between two strands resulting in close helical packing mediated by base-sugar interactions. (B) Comparatively weak interaction involving C<sub>549</sub>·G<sub>35</sub> ... G<sub>544</sub>·C<sub>501</sub> base pairs (pdb: 1fjg) due to nonavailability of the N2 amino group of G<sub>35</sub> for interaction with the ribose sugar, leading to an opening or “crack” at the interface.



a break in the phosphodiester link due to  $\Delta t$  and consequent local twist angle variations (over- and underwinding). However, the sugar-phosphate backbone flexibility absorbs the conformational changes required to re-establish the backbone linkage and underplays the effects of  $\Delta t$ , leading to observed twist angle variations much less than that anticipated from  $\Delta t$  (Fig. 3). Interestingly, data from MD simulations (present study) and a few X-ray crystal structures indicate possible changes in the P–O5' ( $\alpha$ ) and C5'–C4' ( $\gamma$ ) torsion angles from *gauche*<sup>-</sup> to *gauche*<sup>+</sup>/*trans* and from *gauche*<sup>+</sup> to *trans*, respectively, either in the nucleotides associated with the nWC base pair or in the nucleotides immediately flanking them (Fig. 8). The possible direct or indirect significance of these as a structural or functional requirement is not clear.

Earlier attempts at quantifying base-pair nonisostericity (Walberer et al. 2003; Stombaugh et al. 2009) have been used to infer base-pair conformations of nWC pairs (Gautheret and Gutell 1997; Walberer et al. 2003; Mokdad and Frankel 2008), RNA sequence (Stombaugh et al. 2011), and structure alignments (Mokdad and Leontis 2006) in identification (Sarver et al. 2008; Zhong et al. 2010) and clustering

(Zhong and Zhang 2012) of RNA structural motifs. Base-pair isostericity characterized based on the differences in C1' ... C1' separations ( $\Delta c$ ) (Stombaugh et al. 2009) can be related to  $\Delta r$  by a factor of two (half of the difference in the intra-base pair C1' ... C1' distance). Relative displacements of C1' atoms ( $t_1$ ) (Stombaugh et al. 2009) and shear (Olson et al. 2001) are relatable to residual twist ( $\Delta t$ ). Both of these are concurrently accounted for in the circular representation. For instance, the isodiscrepancy index of G.C/G.U (2.14) and U.G/G.U (4.48) pairs (Stombaugh et al. 2009) is roughly proportional to the magnitude of  $\Delta t$  at G.C/G.U (+14.0°) and U.G/G.U (+24.9°). Though correlation between isodiscrepancy index and  $\Delta t$  seemingly draws parallels between the two metric schemes, such straightforward relation may not hold true for other base-pair combinations wherein both  $\Delta t$  and  $\Delta r$  influence nonisostericity. For example, the isodiscrepancy index of G.A/G.C (3.49) and C.U/G.C (3.44) (Stombaugh et al. 2009) does not allow envisioning its effect either through local (helical twist angle variation) or global (kink or bend) conformation of RNA structure. It merely gives a measure to comprehend the extent of nonisostericity

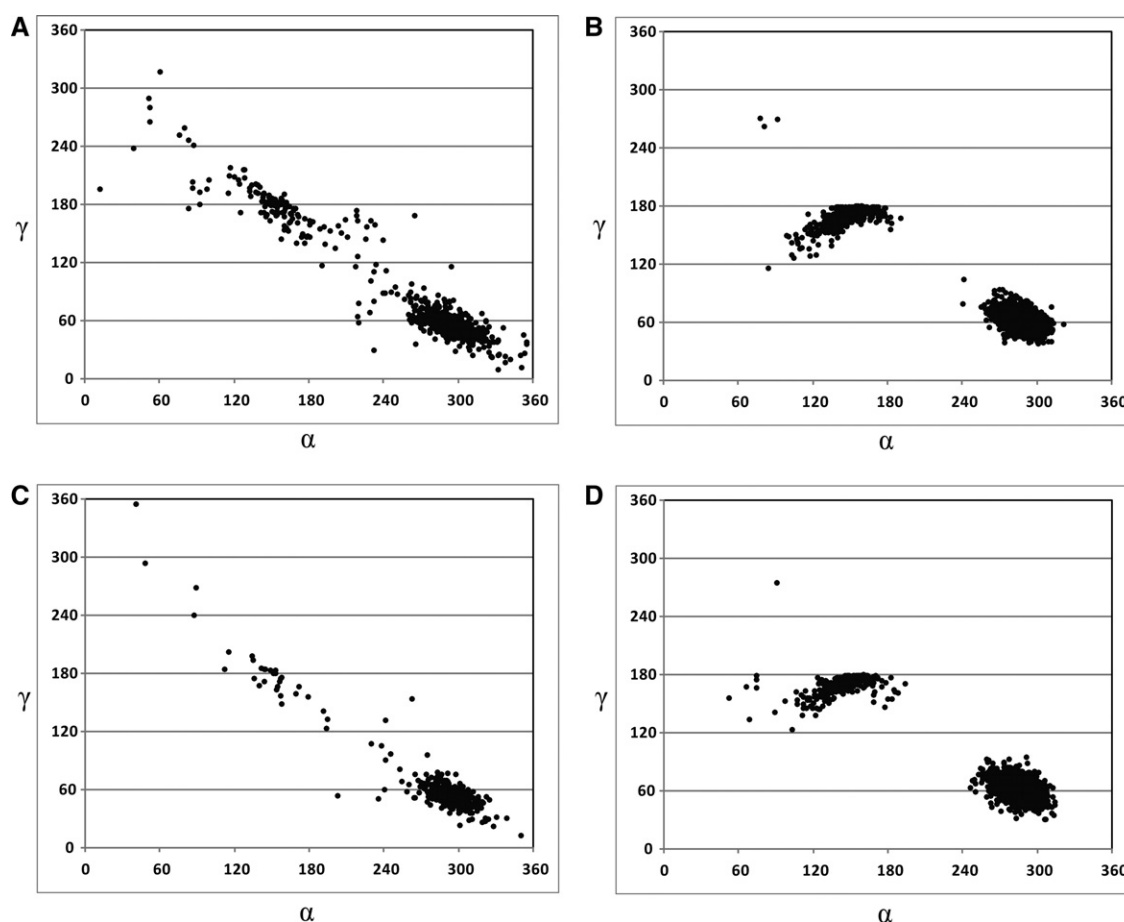


**FIGURE 8.** Correlated backbone conformational variations. Scatter plots depicting conformational changes in the backbone torsion angles,  $\alpha$  (P–O5') and  $\gamma$  (C5'–C4') in nucleotides associated with wobble base pairs (A,B) and in the nucleotides immediately flanking them (C,D). *Left* (A,C) and *right* (B,D) panels correspond to data obtained from crystal and MD simulation structures, respectively.



between two base pairs. In contrast, the distinct measures of base-pair nonisostericity metrics,  $\Delta t$  and  $\Delta r$ , directly relate the cause and effect, providing readily discernible means to base-pair nonisostericity-mediated mechanistic effects. It is noteworthy that nWC base pairs such as C-U and G-A display intrinsic residual twists of  $\Delta t \approx -8.3^\circ$  and  $+7.8^\circ$  respectively, with WC base pairs despite the absence of shear (Fig. 9), further highlighting the usefulness of describing base-pair nonisostericity through circular representation. This seems natural since a circular strip is part of a cylindrical helix.

The base-pair nonisostericity metric discussed here is applicable in principle to all *cis*-nWC base-pair combinations (Table 1). It is seen that certain nWC base pairs such as  $U_h \cdot U_L$  and  $C \cdot C^+$  exhibit a large  $\Delta t$  with the WC pair, while similar large values of  $\Delta t$  are also observed among nWC pairs such as  $C \cdot C^+ / G \cdot U$ ,  $U_h \cdot U_L / G \cdot A$ ,  $A_L \cdot A_h / U_h \cdot U_L$ ,  $C \cdot C^+ / A_L \cdot A_h$ . Likewise, pronounced  $\Delta r$  values are observed for nWC pairs such as G-A, A-A, U-U,  $C \cdot C^+$ , U-C with respect to the WC pair (Table 1). Such large values of  $\Delta t$  and  $\Delta r$  are expected to significantly affect RNA conformations. These might be relevant for protein recognition interactions, as nWC pairs like U-U, U-C, C-C, A-A are involved in trinucleotide repeat expansion diseases (Gatchel and Zoghbi 2005) such as myotonic dystrophy (Kumar et al. 2011), fragile X syndrome E (Kilizek et al. 2012), Huntington's disease, dentatorubral-pallidolusian ataxias (Kilizek et al. 2010). Besides  $\Delta t$ , one might also expect  $\Delta r$  to play a significant role on the global conformation of RNA duplexes comprising purine-purine or pyrimidine-pyrimidine pairs. Thus,  $\Delta t$  and  $\Delta r$  would aid in understanding sequence-dependent RNA conformations arising out of nonisostericity of base pairs.

The scheme is readily extendable to study the effects of nWC base pairs in DNA duplexes such as G-T wobble and can also be adopted for description of base-pair nonisostericity among *trans*-H/SE base pairs (Table 4). Efficacy of the concept of residual twist in predicting mechanistic effects of base triplet nonisostericity in DNA triplexes has been demonstrated (Thenmalarchelvi and Yathindra 2005, 2006) and has been applied in developing an algorithm to identify triplex-forming sequences (Lexa et al. 2011). It is envisaged that the knowledge

of residual twist and radial difference can be effectively utilized for a comprehensive understanding of the structural influence of base-pair nonisostericity in nucleic acids duplexes/triplexes.

## MATERIALS AND METHODS

### Modeling of Watson-Crick and non-Watson-Crick base pairs

Watson-Crick and non-Watson-Crick *cis* base pairs are modeled using standard hydrogen bond length and angles and paired via

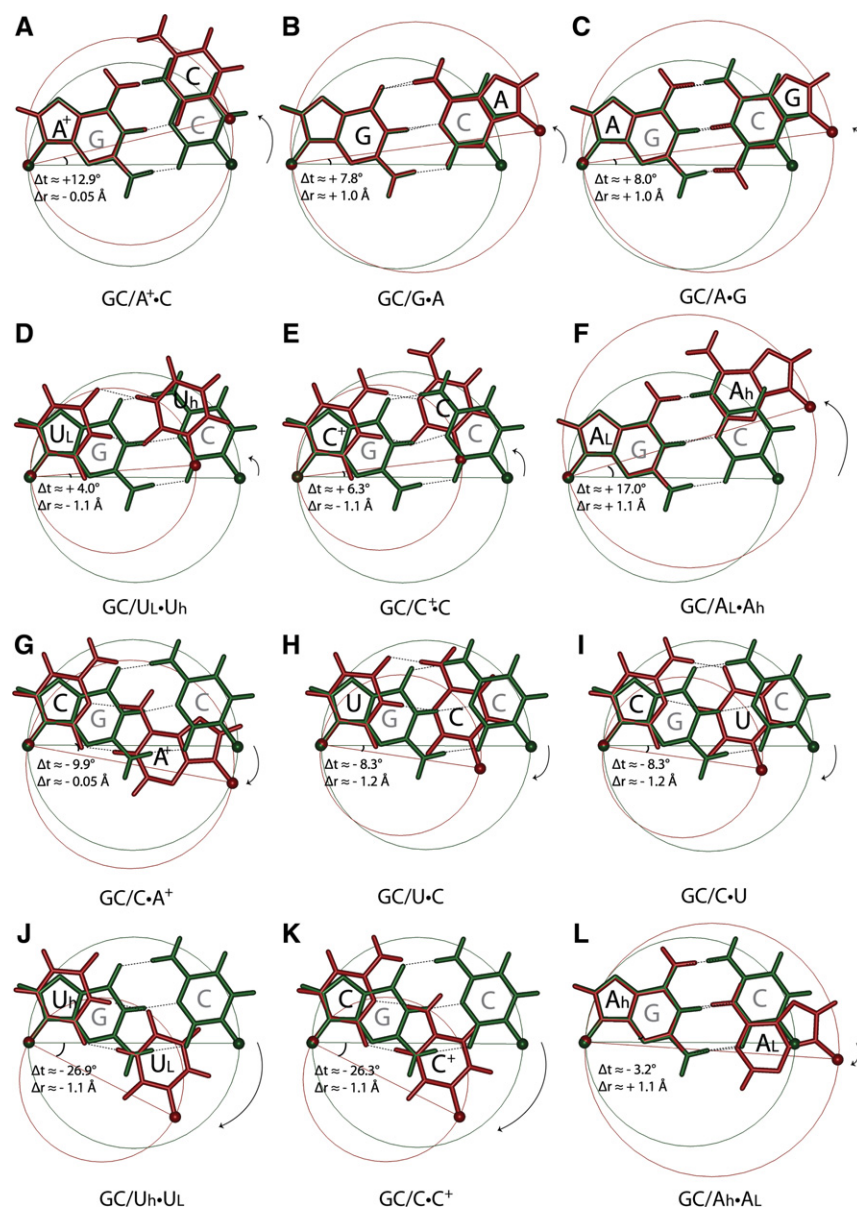


**FIGURE 9.** Visualization of nonisostericity between WC and nWC base pairs. Superposition of various nWC base pairs (brown) on a G.C base pair (representative of WC pairs; green). Base pairs are encompassed by circles with the respective  $C1' \dots C1'$  separation as diameters.  $+\Delta t$  in A–F and  $-\Delta t$  in G–L suggest local overwinding and underwinding, respectively.

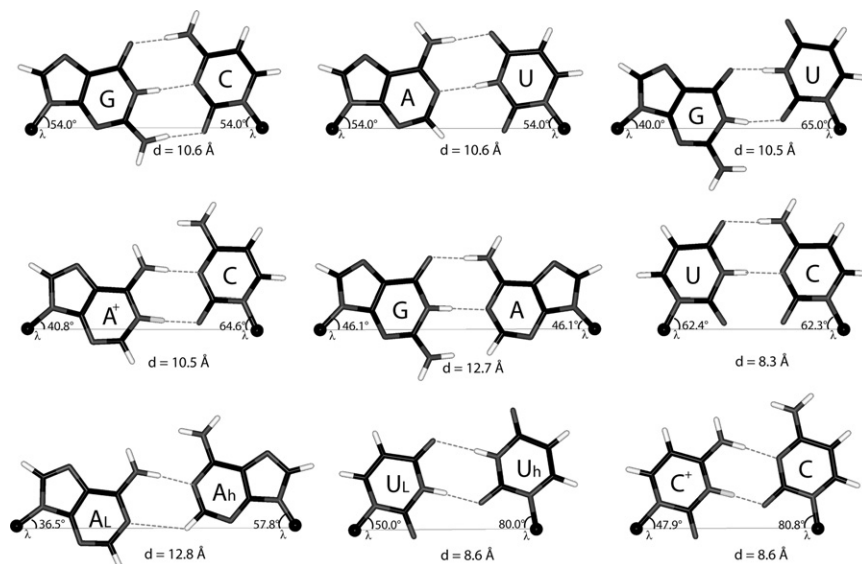


**FIGURE 10.** *cis*-WC and -nWC base pairs. C1' ... C1' separations ( $d$ ) and glycosidic bond angles ( $\lambda$ ) are used to describe various *cis*-WC and *cis*-nWC pairs (Leontis et al. 2002). Bases A and U with high  $\lambda$ -value are designated A<sub>h</sub> and U<sub>h</sub>, respectively.

schemes suggested by Leontis et al. (2002). Glycosidic bond angles ( $\lambda$ ) and the C1' ... C1' separations ( $d$ ) of all modeled base pairs are shown in Figure 10. Base pairs are modeled using the graphical interface of Insight II (Accelrys Inc.).

### Base-pair superposition

Base-pair superposition is achieved by aligning C1', N9, C8, C4/C1', N1, C6, C2 atoms of purines/pyrimidines using the graphical interface of Insight II (Accelrys Inc.).

### Definition of residual twist ( $\Delta t$ ) and radial difference ( $\Delta r$ )

Residual twist ( $\Delta t$ ) is calculated by measuring the angle between the line joining C1' ... C1' atoms of the superimposed base pairs when the helical twist angle ( $t$ ) required to generate a helical structure is not effected, i.e., when  $t = 0$ . The residual twist angle subtended by the 3' base pair in the counter-clockwise direction with respect to the 5' base pair is assigned a positive value and likewise, the residual twist angle subtended by the 3' base pair in the clockwise direction with respect to the 5' base pair is assigned a negative value. The radial difference ( $\Delta r$ ) corresponds to half of the difference between the C1' ... C1' separations (diameter) of the superposed base pairs.  $\Delta r$  is assigned a positive sign if the radius of the 3' base pair is greater than the radius of the 5' base pair and negative sign if the radius of the 3' base pair is less than the radius of the 5' base pair.

### Crystal structure data mining

Crystal structures of RNA duplexes used in the analysis are selected from a list of nonredundant RNA structures (resolution  $\leq 3 \text{ \AA}$ ) from the RNA 3D Hub (<http://rna.bgsu.edu/nrlist/>; Feb. 2012 release). 3D coordinates are retrieved from NDB (Berman et al. 1992) and PDB

(Berman et al. 2000). Instances of helix-loop regions from crystal structures were obtained from RNA FRABASE 2.0 (Popenda et al. 2010). Crystal structure data on protein-RNA interaction involving G-U wobble pairs were obtained from the Protein-RNA Interface Database (PRIDB) v 1.0 (Lewis et al. 2011) and manually curated.

### MD simulation

RNA duplex models comprising wobble pair G-U, U-G (9-mers) and tandem repeats G-U/U-G, U-G/G-U, and G-U/G-U (10-mers) are built using the Discovery studio 2.5 package (Accelrys Inc.) and optimized using the steepest descent algorithm embedded in the package. They are used as the starting model for MD simulations. Using the LEaP module of AMBER 11, RNA duplexes are solvated in a periodic box of TIP3P waters, and neutralizing Na<sup>+</sup> counter ions were added. The equilibration and production runs are pursued following the protocols described in <http://ambermd.org/tutorials/basic/tutorial1>.

Production runs are carried out using the Sander module of AMBER11 for 20 nsec on a high-performance computing cluster (dual hexacore, seven nodes). Simulation is performed under isobaric and isothermal conditions with SHAKE (tolerance = 0.0005  $\text{\AA}$ ) on the hydrogens (Ryckaert et al. 1977), with a 2-fsec integration time and a cut-off distance of 9  $\text{\AA}$  for Lennard-Jones interaction. Trajectories are analyzed using the Ptraj module of AMBER11.

### Calculation of helical twist and backbone torsion angles

Helical twist angle and backbone torsions were estimated using X3DNA (Lu and Olson 2003). Snapshots taken at every 200 psec of MD simulation (Schemes A1 to A5) were used in the calculation. In conformity with the concept of residual twist, helical twist angles are calculated using C1' ... C1' vectors.

### ACKNOWLEDGMENTS

We thank the reviewers for their critical comments and suggestions which significantly enhanced the scope of the article. This work is supported by an institutional grant from the Department of Electronics and Information Technology (DeitY), Government of India, to IBAB under the Centre of Excellence for research and teaching in Bioinformatics. We also thank BRAF-CDAC, Pune for computational resources.

### REFERENCES

- Allain FH, Varani G. 1995. Divalent metal ion binding to a conserved wobble pair defining the upstream site of cleavage of group I self-splicing introns. *Nucleic Acids Res* **23**: 341–350.  
 Auffinger P, Westhof E. 1998. Hydration of RNA base pairs. *J Biomol Struct Dyn* **16**: 693–707.

- Baeyens KJ, De Bondt HL, Pardi A, Holbrook SR. 1996. A curved RNA helix incorporating an internal loop with G·A and A·A non-Watson-Crick base pairing. *Proc Natl Acad Sci* **93**: 12851–12855.
- Berman HM, Olson WK, Beveridge DL, Westbrook J, Gelbin A, Demeny T, Hsieh SH, Srinivasan AR, Schneider B. 1992. The nucleic acid database. A comprehensive relational database of three-dimensional structures of nucleic acids. *Biophys J* **63**: 751–759.
- Berman HM, Westbrook J, Feng Z, Gilliland G, Bhat TN, Weissig H, Shindyalov IN, Bourne PE. 2000. The Protein Data Bank. *Nucleic Acids Res* **28**: 235–242.
- Biswas R, Sundaralingam M. 1997. Crystal structure of r(GUGUGUA)dC with tandem G·U/U·G wobble pairs with strand slippage. *J Mol Biol* **270**: 511–519.
- Biswas R, Wahl MC, Ban C, Sundaralingam M. 1997. Crystal structure of an alternating octamer r(GUAUGUA)dC with adjacent G·U wobble pairs. *J Mol Biol* **267**: 1149–1156.
- Burkard ME, Kierzek R, Turner DH. 1999. Thermodynamics of unpaired terminal nucleotides on short RNA helices correlates with stacking at helix termini in larger RNAs. *J Mol Biol* **290**: 967–982.
- Case DA, Darden TA, Cheatham TE III, Simmerling CL, Wang J, Duke RE, Luo R, Walker RC, Zhang W, Merz KM, et al. 2010. *AMBER 11*. University of California, San Francisco, CA.
- Chang KY, Varani G, Bhattacharya S, Choi H, McClain WH. 1999. Correlation of deformability at a tRNA recognition site and aminoacylation specificity. *Proc Natl Acad Sci* **96**: 11764–11769.
- Correll CC, Wool IG, Munishkin A. 1999. The two faces of the *Escherichia coli* 23 S rRNA sarcin/ricin domain: The structure at 1.11 Å resolution. *J Mol Biol* **292**: 275–287.
- Crick FH. 1966. Codon–anticodon pairing: The wobble hypothesis. *J Mol Biol* **19**: 548–555.
- Deng J, Sundaralingam M. 2000. Synthesis and crystal structure of an octamer RNA r(guguuuac)/r(guaggcac) with G·G/U·U tandem wobble base pairs: Comparison with other tandem G·U pairs. *Nucleic Acids Res* **28**: 4376–4381.
- Ellis JJ, Jones S. 2008. Evaluating conformational changes in protein structures binding RNA. *Proteins* **70**: 1518–1526.
- Frankel AD, Smith CA. 1998. Induced folding in RNA–protein recognition: More than a simple molecular handshake. *Cell* **92**: 149–151.
- Gagnon MG, Steinberg SV. 2002. GU receptors of double helices mediate tRNA movement in the ribosome. *RNA* **8**: 873–877.
- Gagnon MG, Steinberg SV. 2010. The adenosine wedge: A new structural motif in ribosomal RNA. *RNA* **16**: 375–381.
- Gagnon MG, Mukhopadhyay A, Steinberg SV. 2006. Close packing of helices 3 and 12 of 16 S rRNA is required for the normal ribosome function. *J Biol Chem* **281**: 39349–39357.
- Gagnon MG, Boutorine YI, Steinberg SV. 2010. Recurrent RNA motifs as probes for studying RNA–protein interactions in the ribosome. *Nucleic Acids Res* **38**: 3441–3453.
- Gatchel JR, Zoghbi HY. 2005. Diseases of unstable repeat expansion: Mechanisms and common principles. *Nat Rev Genet* **6**: 743–755.
- Gautheret D, Gutell RR. 1997. Inferring the conformation of RNA base pairs and triples from patterns of sequence variation. *Nucleic Acids Res* **25**: 1559–1564.
- Gautheret D, Konings D, Gutell RR. 1995. G·U base pairing motifs in ribosomal RNA. *RNA* **1**: 807–814.
- Gutell RR, Larsen N, Woese CR. 1994. Lessons from an evolving rRNA: 16S and 23S rRNA structures from a comparative perspective. *Microbiol Rev* **58**: 10–26.
- He L, Kierzek R, SantaLucia J Jr, Walter AE, Turner DH. 1991. Nearest-neighbor parameters for G·U mismatches: 5'GU3'/3'UG5' is destabilizing in the contexts CGUG/GUGC, UGUA/AUGU, and AGUU/UUGA but stabilizing in GGUC/CUGG. *Biochemistry* **30**: 11124–11132.
- Hermann T, Westhof E. 1999. Non-Watson–Crick base pairs in RNA–protein recognition. *Chem Biol* **6**: R335–R343.
- Hou YM, Schimmel P. 1988. A simple structural feature is a major determinant of the identity of a transfer RNA. *Nature* **333**: 140–145.
- Huang DB, Vu D, Cassidy LA, Zimmerman JM, Maher LJ III, Ghosh G. 2003. Crystal structure of NF-κB (p50)<sub>2</sub> complexed to a high-affinity RNA aptamer. *Proc Natl Acad Sci* **100**: 9268–9273.
- Jucker FM, Heus HA, Yip PF, Moors EH, Pardi A. 1996. A network of heterogeneous hydrogen bonds in GNRA tetraloops. *J Mol Biol* **264**: 968–980.
- Kiliszek A, Kierzek R, Krzyzosiak WJ, Rypniewski W. 2010. Atomic resolution structure of CAG RNA repeats: Structural insights and implications for the trinucleotide repeat expansion diseases. *Nucleic Acids Res* **38**: 8370–8376.
- Kiliszek A, Kierzek R, Krzyzosiak WJ, Rypniewski W. 2012. Crystallographic characterization of CCG repeats. *Nucleic Acids Res* **40**: 8155–8162.
- Klein DJ, Schmeing TM, Moore PB, Steitz TA. 2001. The kink-turn: A new RNA secondary structure motif. *EMBO J* **20**: 4214–4221.
- Kumar A, Park H, Fang P, Parkesh R, Guo M, Nettles KW, Disney MD. 2011. Myotonic dystrophy type 1 RNA crystal structures reveal heterogeneous 1 × 1 nucleotide UU internal loop conformations. *Biochemistry* **50**: 9928–9935.
- Ladner JE, Jack A, Robertus JD, Brown RS, Rhodes D, Clark BF, Klug A. 1975. Structure of yeast phenylalanine transfer RNA at 2.5 Å resolution. *Proc Natl Acad Sci* **72**: 4414–4418.
- Lee JC, Gutell RR. 2004. Diversity of base-pair conformations and their occurrence in rRNA structure and RNA structural motifs. *J Mol Biol* **344**: 1225–1249.
- Leonard GA, McAuley-Hecht KE, Ebel S, Lough DM, Brown T, Hunter WN. 1994. Crystal and molecular structure of r(CGCGAAUUAGCG): An RNA duplex containing two G(anti)·A(anti) base pairs. *Structure* **2**: 483–494.
- Leontis NB, Westhof E. 2001. Geometric nomenclature and classification of RNA base pairs. *RNA* **7**: 499–512.
- Leontis NB, Stombaugh J, Westhof E. 2002. The non-Watson–Crick base pairs and their associated isostericity matrices. *Nucleic Acids Res* **30**: 3497–3531.
- Lewis BA, Walia RR, Terribilini M, Ferguson J, Zheng C, Honavar V, Dobbs D. 2011. PRIDB: A Protein–RNA Interface Database. *Nucleic Acids Res* **39**: D277–D282.
- Lexa M, Martinek T, Burgetová I, Kopeček D, Brázdrová M. 2011. A dynamic programming algorithm for identification of triplex-forming sequences. *Bioinformatics* **27**: 2510–2517.
- Lu XJ, Olson WK. 2003. 3DNA: A software package for the analysis, rebuilding and visualization of three-dimensional nucleic acid structures. *Nucleic Acids Res* **31**: 5108–5121.
- Masquida B, Westhof E. 2000. On the wobble GoU and related pairs. *RNA* **6**: 9–15.
- McClain WH, Foss K. 1988. Changing the identity of a tRNA by introducing a G·U wobble pair near the 3' acceptor end. *Science* **240**: 793–796.
- Mizuno H, Sundaralingam M. 1978. Stacking of Crick Wobble pair and Watson–Crick pair: Stability rules of G·U pairs at ends of helical stems in tRNAs and the relation to codon–anticodon Wobble interaction. *Nucleic Acids Res* **5**: 4451–4461.
- Mládek A, Sharma P, Mitra A, Bhattacharyya D, Sponer J, Sponer JE. 2009. Trans Hoogsteen/sugar edge base pairing in RNA. Structures, energies, and stabilities from quantum chemical calculations. *J Phys Chem B* **113**: 1743–1755.
- Mokdad A, Frankel AD. 2008. ISFOLD: Structure prediction of base pairs in non-helical RNA motifs from isostericity signatures in their sequence alignments. *J Biomol Struct Dyn* **25**: 467–472.
- Mokdad A, Leontis NB. 2006. Ribostral: An RNA 3D alignment analyzer and viewer based on basepair isosterisities. *Bioinformatics* **22**: 2168–2170.
- Mueller U, Schübel H, Sprinzl M, Heinemann U. 1999. Crystal structure of acceptor stem of tRNA<sup>Ala</sup> from *Escherichia coli* shows unique G·U wobble base pair at 1.16 Å resolution. *RNA* **5**: 670–677.
- Nagaswamy U, Larios-Sanz M, Hury J, Collins S, Zhang Z, Zhao Q, Fox GE. 2002. NCIR: A database of non-canonical interactions in known RNA structures. *Nucleic Acids Res* **30**: 395–397.



- Nissen P, Ippolito JA, Ban N, Moore PB, Steitz TA. 2001. RNA tertiary interactions in the large ribosomal subunit: The A-minor motif. *Proc Natl Acad Sci* **98**: 4899–4903.
- Olson WK, Bansal M, Burley SK, Dickerson RE, Gerstein M, Harvey SC, Heinemann U, Lu XJ, Neidle S, Shakked Z, et al. 2001. A standard reference frame for the description of nucleic acid base-pair geometry. *J Mol Biol* **313**: 229–237.
- Park SJ, Hou YM, Schimmel P. 1989. A single base pair affects binding and catalytic parameters in the molecular recognition of a transfer RNA. *Biochemistry* **28**: 2740–2746.
- Peebles CL, Zhang M, Perlman PS, Franzen JS. 1995. Catalytically critical nucleotide in domain 5 of a group II intron. *Proc Natl Acad Sci* **92**: 4422–4426.
- Popenda M, Szachniuk M, Blazewicz M, Wasik S, Burke EK, Blazewicz J, Adamiak RW. 2010. RNA FRABASE 2.0: An advanced web-accessible database with the capacity to search the three-dimensional fragments within RNA structures. *BMC Bioinformatics* **11**: 231–242.
- Pütz J, Puglisi JD, Florentz C, Giegé R. 1991. Identity elements for specific aminoacylation of yeast tRNA<sup>Asp</sup> by cognate aspartyl-tRNA synthetase. *Science* **252**: 1696–1699.
- Quigley GJ, Seeman NC, Wang AH, Suddath FL, Rich A. 1975. Yeast phenylalanine transfer RNA: Atomic coordinates and torsion angles. *Nucleic Acids Res* **2**: 2329–2341.
- Ryckaert JP, Ciccotti G, Berendsen HJC. 1977. Numerical integration of the Cartesian equations of motion of a system with constraints: Molecular dynamics of *n*-alkanes. *J Comp Phys* **23**: 327–341.
- Saenger W. 1984. *Principles of nucleic acid structure*. Springer-Verlag, New York.
- Sarver M, Zirbel CL, Stombaugh J, Mokdad A, Leontis NB. 2008. FR3D: Finding local and composite recurrent structural motifs in RNA 3D structures. *J Math Biol* **56**: 215–252.
- Serra MJ, Lyttle MH, Axenson TJ, Schadt CA, Turner DH. 1993. RNA hairpin loop stability depends on closing base pair. *Nucleic Acids Res* **21**: 3845–3849.
- Stombaugh J, Zirbel CL, Westhof E, Leontis NB. 2009. Frequency and isostericity of RNA base pairs. *Nucleic Acids Res* **37**: 2294–2312.
- Stombaugh J, Widmann J, McDonald D, Knight R. 2011. Boulder ALIGNment Editor (ALE): A web-based RNA alignment tool. *Bioinformatics* **27**: 1706–1707.
- Stout CD, Mizuno H, Rubin J, Brennan T, Rao ST, Sundaralingam M. 1976. Atomic coordinates and molecular conformation of yeast phenylalanyl tRNA. An independent investigation. *Nucleic Acids Res* **3**: 1111–1123.
- Strobel SA, Cech TR. 1995. Minor groove recognition of the conserved G-U pair at the *Tetrahymena* ribozyme reaction site. *Science* **267**: 675–679.
- Szewczak AA, Moore PB, Chang YL, Wool IG. 1993. The conformation of the sarcin/ricin loop from 28S ribosomal RNA. *Proc Natl Acad Sci* **90**: 9581–9585.
- Szymański M, Barciszewska MZ, Erdmann VA, Barciszewski J. 2000. An analysis of G-U base pair occurrence in eukaryotic 5S rRNAs. *Mol Biol Evol* **17**: 1194–1198.
- Thenmalarchelvi R, Yathindra N. 2005. New insights into DNA triplexes: Residual twist and radial difference as measures of base triplet non-isomorphism and their implication to sequence-dependent non-uniform DNA triplex. *Nucleic Acids Res* **33**: 43–55.
- Thenmalarchelvi R, Yathindra N. 2006. Base triplet nonisomorphism strongly influences DNA triplex conformation: Effect of nonisomorphic G\*GC and A\*AT triplets and bending of DNA triplexes. *Biopolymers* **82**: 443–461.
- van Knippenberg PH, Formenoy LJ, Heus HA. 1990. Is there a special function for U.G basepairs in ribosomal RNA? *Biochim Biophys Acta* **1050**: 14–17.
- Varani G, McClain WH. 2000. The G-U wobble base pair. A fundamental building block of RNA structure crucial to RNA function in diverse biological systems. *EMBO Rep* **1**: 18–23.
- Walberer BJ, Cheng AC, Frankel AD. 2003. Structural diversity and isomorphism of hydrogen-bonded base interactions in nucleic acids. *J Mol Biol* **327**: 767–780.
- Walter AE, Wu M, Turner DH. 1994. The stability and structure of tandem GA mismatches in RNA depend on closing base pairs. *Biochemistry* **33**: 11349–11354.
- Weeks KM, Crothers DM. 1993. Major groove accessibility of RNA. *Science* **261**: 1574–1577.
- Wimberly B, Varani G, Tinoco I Jr. 1993. The conformation of loop E of eukaryotic 5S ribosomal RNA. *Biochemistry* **32**: 1078–1087.
- Wu M, McDowell JA, Turner DH. 1995. A periodic table of symmetric tandem mismatches in RNA. *Biochemistry* **34**: 3204–3211.
- Xu D, Landon T, Greenbaum NL, Fenley MO. 2007. The electrostatic characteristics of G-U wobble base pairs. *Nucleic Acids Res* **35**: 3836–3847.
- Zhong C, Zhang S. 2012. Clustering RNA structural motifs in ribosomal RNAs using secondary structural alignment. *Nucleic Acids Res* **40**: 1307–1317.
- Zhong X, Leontis N, Qian S, Itaya A, Qi Y, Boris-Lawrie K, Ding B. 2006. Tertiary structural and functional analyses of a viroid RNA motif by isostericity matrix and mutagenesis reveal its essential role in replication. *J Virol* **80**: 8566–8581.
- Zhong C, Tang H, Zhang S. 2010. RNAMotifScan: Automatic identification of RNA structural motifs using secondary structural alignment. *Nucleic Acids Res* **38**: e176.





# RNA

A PUBLICATION OF THE RNA SOCIETY

## An innate twist between Crick's wobble and Watson-Crick base pairs

Prakash Ananth, Gunaseelan Goldsmith and Narayanarao Yathindra

RNA 2013 19: 1038-1053

---

### References

This article cites 76 articles, 21 of which can be accessed free at:  
<http://rnajournal.cshlp.org/content/19/8/1038.full.html#ref-list-1>

### Creative Commons License

This article is distributed exclusively by the RNA Society for the first 12 months after the full-issue publication date (see <http://rnajournal.cshlp.org/site/misc/terms.xhtml>). After 12 months, it is available under a Creative Commons License (Attribution-NonCommercial 3.0 Unported), as described at <http://creativecommons.org/licenses/by-nc/3.0/>.

### Email Alerting Service

Receive free email alerts when new articles cite this article - sign up in the box at the top right corner of the article or [click here](#).

---



---

To subscribe to *RNA* go to:  
<http://rnajournal.cshlp.org/subscriptions>

---